ELSEVIER

Journal of Organometallic Chemistry 498 (1995) 257–266

Journal of Organometallic Chemistry

Seven-coordinate complexes of molybdenum(II) and tungsten(II) containing pyridine-2-thionate and pyrimidine-2-thionate. Crystal structure of $[W(CO)_3(\eta^2\text{-pymS})_2]$ (pymS = pyrimidine-2-thionate)

Paul K. Baker [a,*], Mary E. Harman [b], Steven Hughes [a], Michael B. Hursthouse [b], K.M. Abdul Malik [b]

[a] *Department of Chemistry, University of Wales, Bangor, Gwynedd, LL57 2UW, UK*
[b] *Department of Chemistry, University of Wales Cardiff, PO Box 912, Cardiff, CF1 3TB, UK*

Received 13 February 1995

Abstract

Reaction of $[WI_2(CO)_3(NCMe)_2]$ with two equivalents of K[pymS] (pymS = pyrimidine-2-thionate) has given the crystallographically characterised complex $[W(CO)_3(\eta^2\text{-pymS})_2]$ (**1**). The structure can be described as a distorted monocapped trigonal prism with a carbonyl ligand in the unique capping position. Equimolar quantities of $[MI_2(CO)_3(NCMe)_2]$ and L {for M = Mo or W, L = PPh_3; for M = W only, L = PPh_2Cy or PPh_2Nap (Nap = napthyl)} react to give $[MI_2(CO)_3(NCMe)L]$, followed by reaction in situ with K[pyS or pymS] (pyS = pyridine-2-thionate) afforded the complexes $[MI(CO)_3L(\eta^2\text{-pyS or pymS})]$ (**2–7**). The tungsten complexes $[WI_2(CO)_3LL']$ {L = L' = PPh_3, PPh_2Cy, PPh_2Nap or L = $PPhBz_2$, L' = $AsPh_3$; L = PPh_3, L' = PPh_2Bz, $PPhBz_2$, $AsPh_3$ or $SbPh_3$} (prepared in situ) react with an equimolar amount of K[pymS] to give the S-monodentately coordinated pyrimidine-2-thionate complexes $[WI(CO)_3LL'(\eta^1\text{-S-pymS})]$ (**8–15**). Similarly, treatment of $[WI_2(CO)_3\{Ph_2P(CH_2)_nPPh_2\}]$ (n = **1–6**) (prepared in situ) with one equivalent of K[pyS] or K[pymS] yielded the monodentately attached pyrimidine-2-thionate or pyridine-2-thionate complexes $[WI(CO)_3\{Ph_2P(CH_2)_nPPh_2\}(\eta^1\text{-S-pyS or -S-pymS})]$ (**16–27**). The molybdenum complex $[MoI_2(CO)_3\{Ph_2P(CH_2)_2PPh_2\}]$ (prepared in situ) reacts with an equimolar amount of K[pymS] to give the bidentately coordinated pyrimidine-2-thionate dicarbonyl complex $[MoI(CO)_2\{Ph_2P(CH_2)_2PPh_2\}(\eta^2\text{-pymS})]$ (**28**).

Keywords: Molybdenum(II); Tungsten(II); Seven-coordinate; Pyridine-2-thionate; Pyrimidine-2-thionate; Crystal structure

1. Introduction

Transition-metal complexes containing 1,1-dithiolates have received considerable attention over the years [1–3]. The coordination chemistry of the related heterocyclic thionate ligands, pyridine-2-thionate and pyrimidine-2-thionate have also been studied. For example, the pyridine-2-thionate has been shown to adopt a variety of coordination modes, namely, (a) S-monodentate [4,5], (b) S,N-chelating [4–6], (c) S,N-bridging [7] and (d) S-monodentate, with a weak M · · · N interaction [8]. Some previously reported monomeric molybdenum(II) and tungsten(II) seven-coordinate pyridine-2-thiolate (pyS) complexes [9] are the S,N-chelating complexes $[M(CO)_3(\eta^2\text{-pyS})_2]$ (M = Mo or W) and $[M(CO)_2(PMe_2Ph)(\eta^2\text{-pyS})_2]$ (M = Mo or W) which was crystallographically characterised for M = W. The tricarbonyl complexes $[M(CO)_3(\eta^2\text{-pyS})_2]$ reported by Deeming et al. [9] were prepared in low yield by treating the zero-valent complexes *fac*-$[M(CO)_3(NCMe)_3]$ with pySH in acetonitrile.

In order to obtain higher yields and expand the range of molybdenum(II) and tungsten(II) complexes and bonding modes of pyridine-2-thionate and pyrimidine-2-thionate we have carried out a study of the reactions of the seven-coordinate complexes $[MI_2(CO)_3(NCMe)_2]$ (M = Mo or W) and their derivatives with potassium pyridine-2-thionate and potassium pyrimidine-2-thionate and the results are described below. The molecular

* Corresponding author.

SSDI 0022-328X(95)05532-0

structure of the bis(pyrimidine-2-thionate) complex $[W(CO)_3(\eta^2\text{-pymS})_2]$ is also reported.

2. Results and discussion

The starting materials used in this research, $[MI_2(CO)_3(NCMe)_2]$ (M = Mo or W) were prepared [10] by treating the zero-valent complexes *fac*-$[M(CO)_3(NCMe)_3]$ (prepared in situ [11]) with an equimolar amount of I_2 at 0°C. The reaction of $[WI_2(CO)_3(NCMe)_2]$ with two equivalents of K[pymS] in CH_2Cl_2 at room temperature afforded the iodide- and acetonitrile-displaced seven-coordinate complex $[W(CO)_3(\eta^2\text{-pymS})_2]$ (**1**) in good yield. This complex was characterised by elemental analysis (C, H and N) (Table 1), IR (Table 2) and ^1H NMR spectroscopy (Table 3) and also by X-ray crystallography (Fig. 1). It is soluble in acetone and chlorinated solvents, but only sparingly soluble in diethyl ether and insoluble in hydrocarbon solvents. Complex (**1**) is stable in the solid state when stored under nitrogen, but it is very air-sensitive in solution. This complex has similar properties to those of the analogous bis(pyridine-2-thionate) complex $[W(CO)_3(\eta^2\text{-pyS})_2]$ reported by Deeming and et al. [9]. The IR spectrum for (**1**) exhibited only two bands in the carbonyl region at 2029 and 1941 cm^{-1}. The lower frequency band results from a degenerative pair of carbonyl stretching vibrations. This is consistent with a facial *cis*-tricarbonyl arrangement in the complex with effective local C_{3v} symmetry. This arrangement, which is identical to that of the related complex, $[W(CO)_3(\eta^2\text{-pyS})_2]$ [9], minimises competition for metal dπ-electron density between the three carbonyl ligands. The ^1H NMR spectrum showed only one set of pymS resonances at room temperature at $\delta = 8.60$ pymS–H^6, 8.45 pymS–H^4 and 6.95 pymS–H^5 ppm (Table 3). The inequivalence of protons H^4 and H^6 is consistent with pymS bonding in the chelate mode, and is as expected for a coordinatively saturated complex that obeys the effective atomic number rule.

Suitable single crystals of (**1**) for X-ray crystallography were grown from a CH_2Cl_2/Et_2O (80:20) solution at −25°C. The molecular structure of (**1**) is shown in Fig. 1 together with the atomic numbering scheme. The atomic coordinates and bond lengths and angles are given in Tables 4 and 5, respectively. The structure of (**1**) has two N,S-chelating pymS ligands and three carbonyl ligands in the facial arrangement. The structure can best be described as a distorted monocapped trigonal prism with a carbonyl ligand, C(9)–O(1), in the unique capping position. One S atom {S(1)}, one N atom {N(2)} and two carbonyl carbon atoms {C(10) and C(11)} occupy the capped quadrilateral face and the other N atom {N(3)} and the other S atom {S(2)} comprise the remaining edge. A coordinatively saturated 18-electron structure is therefore adopted. The S-atoms of the two chelating pymS ligands are approximately *trans* coordinated {144.20(7)°}. The restricted bite distance of the two pymS ligands, which subtend angles at the tungsten centre of 64.38(14)° and 64.7(2)°, constrain the two coordinated N atoms to adopt a *cis*-arrangement {83.2(2)°}. The small bite distances of the two chelating pymS ligands are probably responsible for the preferred distorted capped trigonal prismatic geometry in this structure. The *trans* coordination disposition of the two pymS S-atoms is the more usual arrangement found for transition-metal complexes containing two chelating pyrimidine-2-thionate ligands [12–14]. The W–S bond lengths of 2.536(2) and 2.520(2) Å, respectively, compare with those of 2.538(2) and 2.520(3) Å in the related complex $[W(CO)_2(PMe_2Ph)(\eta^2\text{-pyS})_2]$ [9], and also with average W–S bond lengths of 2.54 Å for bis(dithiocarbamato) tungsten(II) seven-coordinate complexes [15,16]. The two W–S bond lengths are inequivalent; 2.536(2) Å W(1)–S(1) being slightly longer than 2.520(2) Å W(1)–S(2). Similarly, the two W–N bond lengths are also inequivalent with W(1)–N(2) 2.233(6) Å being slightly longer than that of W(1)–N(3) 2.207(5) Å. This may be attributed to the greater *trans* effect of the two noncapping carbonyl ligands C(10)–O(2) and C(11)–O(3) as opposed to that of the capping carbonyl ligand, C(9)–O(1), in this structure. The average S–C bond length of ca. 1.74 Å and C–N bond lengths ca. 1.34 Å, in the pyrimidine-2-thionate ligands, are similar to those observed in other pyrimidine-2-thionate complexes [17,18]. This suggests a delocalised ring structure with a C–N bond order of ca. 1.5 and therefore that these ligands are actually bonded as thiolates, with little contribution from the thione form.

The two pymS ligands are inequivalent in the solid-state structure. However, as described earlier, the room temperature ^1H NMR spectrum of (**1**) showed only one set of pymS resonances. The apparent equivalence of the two pymS ligands in the spectrum at room temperature can be attributed to fluxionality in solution. A similar observation was made by Deeming et al. [9] for the related bis(pyridine-2-thionate) complex $[W(CO)_3(\eta^2\text{-pyS})_2]$. Likewise, the room temperature ^{13}C NMR spectrum (CD_2Cl_2, 298 K) of (**1**) showed only a single carbonyl resonance at $\delta = 231.3$ ppm, which indicates that the three carbonyl ligands are fluxional and probably undergo rapid turnstile rotation about the tungsten atom at 298 K. The ^{13}C NMR spectrum in CD_2Cl_2 at 203 K also only showed one carbonyl resonance and indicated that the molecule was still fluxional at 203 K. The average W–C bond length of 1.99 Å in the solid-state structure is typical for heptacoordinate tungsten(II) tricarbonyl complexes [15]. The average W–C length is longer than that in the related bis(pyridine-2-thionate)dicarbonyl complex $[W(CO)_2(PMe_2Ph)(\eta^2\text{-pyS})_2]$ [9]

Table 1
Physical and analytical data for the pyridine-2-thionate and pyrimidine-2-thionate complexes of molybdenum(II) and tungsten(II)

Complex		Colour	Yield (%)	Analytical data, found (calc.) (%)				
				W [a]	C	H	N	I
1	$[W(CO)_3(\eta^2\text{-pymS})_2]$	Dark brown	76	—	27.0 (27.0)	1.4 (1.2)	11.2 (11.4)	—
2	$[MoI(CO)_3(PPh_3)(\eta^2\text{-pyS})]$	Dark purple–brown	76	—	44.9 (45.9)	3.5 (2.8)	2.4 (2.1)	—
3	$[WI(CO)_3(PPh_3)(\eta^2\text{-pyS})]$	Brown	55	24.2 (24.0)	41.3 (40.7)	3.0 (2.5)	1.5 (1.8)	—
4	$[MoI(CO)_3(PPh_3)(\eta^2\text{-pymS})]$	Dark purple–brown	71	—	43.6 (44.1)	3.2 (2.7)	3.7 (4.1)	—
5	$[WI(CO)_3(PPh_3)(\eta^2\text{-pymS})]$	Brown	61	—	39.8 (39.1)	2.6 (2.4)	3.2 (3.7)	—
6	$[WI(CO)_3(PPh_2Cy)(\eta^2\text{-pymS})]$	Brown	47	—	40.2 (38.8)	3.7 (3.1)	3.5 (3.6)	—
7	$[WI(CO)_3(PPh_2Nap)(\eta^2\text{-pymS})]$	Rust	62	23.3 (22.5)	43.8 (42.6)	3.0 (2.5)	3.4 (3.4)	—
8	$[WI(CO)_3(PPh_3)_2(\eta^1\text{-S-pymS})]$	Orange	50	—	50.1 (50.1)	3.5 (3.2)	2.8 (2.7)	—
9	$[WI(CO)_3(PPh_2Cy)_2(\eta^1\text{-S-pymS})]$	Rust	48	—	48.4 (49.5)	4.6 (4.4)	2.7 (2.7)	—
10	$[WI(CO)_3(PPh_2Nap)_2(\eta^1\text{-S-pymS})]$	Brown	64	—	53.8 (54.2)	3.9 (3.3)	2.4 (2.5)	—
11	$[WI(CO)_3(PPh_3)(PPh_2Bz)(\eta^1\text{-S-pymS})]$	Brown	51	—	50.1 (50.6)	3.6 (3.4)	2.4 (2.7)	—
12	$[WI(CO)_3(PPh_3)(PPhBz_2)(\eta^1\text{-S-pymS})]$	Brown	58	—	50.7 (51.0)	3.8 (3.5)	2.4 (2.6)	—
13	$[WI(CO)_3(PPh_3)(AsPh_3)(\eta^1\text{-S-pymS})]$	Brown	57	—	49.4 (48.1)	3.4 (3.1)	2.3 (2.6)	—
14	$[WI(CO)_3(PPh_3)(SbPh_3)(\eta^1\text{-S-pymS})]$	Dark brown	32	—	47.1 (46.1)	3.6 (3.0)	2.4 (2.5)	—
15	$[WI(CO)_3(PPhBz_2)(AsPh_3)(\eta^1\text{-S-pymS})]$	Brown	48	—	50.0 (50.3)	3.6 (3.5)	2.7 (2.6)	—
16	$[WI(CO)_3(dppm)(\eta^1\text{-S-pyS})]$	Golden-brown	83	—	43.9 (44.6)	3.3 (3.0)	1.8 (1.6)	14.3 (14.3)
17	$[WI(CO)_3(dppm)(\eta^1\text{-S-pymS})] \cdot \frac{1}{2}CH_2Cl_2$	Brown	71	—	42.2 (41.8)	3.0 (2.8)	2.6 (3.0)	—
18	$[WI(CO)_3(dppe)(\eta^1\text{-S-pyS})]$	Orange	89	—	45.6 (45.2)	3.5 (3.1)	1.8 (1.6)	14.6 (14.1)
19	$[WI(CO)_3(dppe)(\eta^1\text{-S-pymS})]$	Gold	48	—	43.7 (43.8)	3.2 (3.0)	3.3 (3.1)	—
20	$[WI(CO)_3(dppp)(\eta^1\text{-S-pyS})]$	Golden-brown	63	—	46.3 (45.8)	3.8 (3.3)	1.8 (1.5)	—
21	$[WI(CO)_3(dppp)(\eta^1\text{-S-pymS})]$	Rust	74	19.2 (20.0)	44.5 (44.5)	3.6 (3.2)	3.3 (3.1)	—
22	$[WI(CO)_3(dppb)(\eta^1\text{-S-pyS})]$	Golden-brown	80	19.6 (19.7)	45.6 (46.4)	3.7 (3.5)	1.6 (1.5)	—
23	$[WI(CO)_3(dppb)(\eta^1\text{-S-pymS})]$	Brown	71	—	45.7 (45.1)	3.7 (3.4)	2.5 (3.0)	13.2 (13.6)
24	$[WI(CO)_3(dppe)(\eta^1\text{-S-pyS})]$	Brown	64	—	47.4 (47.0)	4.2 (3.6)	1.3 (1.5)	—
25	$[WI(CO)_3(dppe)(\eta^1\text{-S-pymS})]$	Dark brown	70	—	46.0 (45.7)	4.0 (3.5)	2.6 (3.0)	—
26	$[WI(CO)_3(dpph)(\eta^1\text{-S-pyS})] \cdot \frac{1}{2}CH_2Cl_2$	Brown	66	—	46.2 (46.2)	4.0 (3.7)	1.6 (1.4)	—
27	$[WI(CO)_3(dpph)(\eta^1\text{-S-pymS})] \cdot \frac{1}{2}CH_2Cl_2$	Brown	82	—	45.5 (44.9)	3.8 (3.6)	3.0 (2.8)	—
28	$[MoI(CO)_2(dppe)(\eta^2\text{-pymS})]$	Brown	43	—	49.5 (48.8)	3.6 (3.5)	3.1 (3.5)	—

[a] Analytical errors, W ≠ ±5%.

which has W–C of 1.95 Å. This was expected since displacement of carbon monoxide by a phosphine would result in decreased competition for available metal $d\pi$ electron density by the carbonyl ligands in the latter and hence lead to increased M–C≡O back-bonding.

The reactions of $[MI_2(CO)_3(NCMe)_2]$ (M = Mo or W) with an equimolar amount of L {for M = Mo or W, L = PPh_3; for M = W only, L = PPh_2Cy or PPh_2Nap} in CH_2Cl_2 at room temperature gave $[MI_2(CO)_3(NCMe)L]$ [19], which when treated in situ with one equivalent of K[pyS] or K[pymS] yielded the new complexes $[MI(CO)_3L(\eta^2\text{-pyS or pymS})]$ (2–7) in good yield. These complexes have been characterised by elemental analysis (C, H, N, or in selected cases W) (Table 1), IR (Table 2) and ^1H NMR spectroscopy (Table 3). Complexes (**2–7**) were fairly stable in the solid-state when kept under dinitrogen, but slowly decomposed in solution when exposed to air. These complexes were all soluble in acetone and dichloromethane but were insoluble in diethyl ether and hydrocarbon solvents. As expected, the majority of these complexes

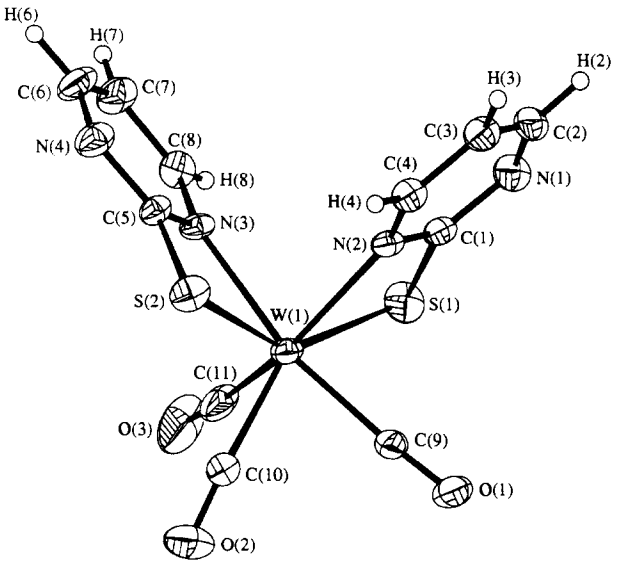

Fig. 1. X-ray crystal structure of $[W(CO)_3(\eta^2\text{-pymS})_2]$ (**1**) together with the atom numbering scheme.

Table 2
IR data (cm^{-1}) [a] for the pyridine-2-thionate and pyrimidine-2-thionate complexes of molybdenum(II) and tungsten(II)

Complex	ν(C≡O)	ν(C=C/C=N) skeletal	ν(C=S)
1	2029s, 1941br,s [b]	1572m	1182m
2	2036m, 1963ms, 1889m	1585m	1153mw
3	2024s, 1944s, 1914ms	1588mw	1147mw
4	2034ms, 1955s, 1879ms	1568m	1186m
5	2026ms, 1947br,ms [b]	1573m	1185m
6	2024s, 1942s, 1920ms,sh	1573mw	1185mw
7	2024s, 1941br,s [b]	1573m	1185m
8	2027m, 1932s, 1856ms	1575mw	1186m
9	2023s, 1942s, 1925sh	1573m	1187m
10	2024s, 1942br,s [b]	1571m	1187m
11	2025s, 1945s, 1857ms	1573m	1186m
12	2025s, 1945s, 1856ms	1573m	1185m
13	2025s, 1934br,s [b]	1573m	1184m
14	2027s, 1948s, 1856m	1574mw	1180sh,m
15	2024s, 1941br,s [b]	1573m	1185m
16	2035m, 1944s, 1869s	1584m	1140mw
17	2033ms, 1952s, 1866s	1572m	1188m
18	2022m, 1940s, 1864ms	1586m	1141mw
19	2027m, 1941s, 1851s	1572m	1187m
20	2023m, 1917s, 1848s	1581m	1140m
21	2024ms, 1940s, 1857ms	1573m	1185m
22	2022m, 1922s, 1846m	1587mw	1145mw
23	2025ms, 1928s, 1853ms	1573m	1185m
24	2021s, 1922s, 1846s	1588m	1145m
25	2023s, 1926s, 1854s	1572ms, 1582sh,m	1185ms
26	2021ms, 1924s, 1847ms	1587m	1144m
27	2026s, 1930s, 1854s	1572m	1186m
28	1957s, 1885s	1571m	1189sh,m

[a] Spectra recorded as thin films in $CHCl_3$ between NaCl plates; br = broad, m = medium, ms = medium-strong, mw = medium-weak, s = strong, sh = shoulder.
[b] Two equivalent ν(C≡O) stretches.

exhibited three bands in the carbonyl region of their IR spectra (Table 2), indicating the presence of three nonequivalent CO ligands in these complexes. The exceptions were complexes (**5**) and (**7**) which both showed only two bands in the carbonyl region, the respective lower frequency vibrations of which were much broader and more intense than in the other complexes and are taken as evidence of the presence of a pair of degenerative CO stretching vibrations in these two complexes. All of these new complexes possessed a skeletal-ring (C=C/C=N) stretching vibration in the expected region, approximately 1570–1585 cm^{-1}. These complexes also showed a thiocarbonyl stretching vibration in the region of 1140–1190 cm^{-1}, suggesting that at least some contribution to bonding in the thionate form of the pyS or pymS ligands [20]. The ^1H NMR spectra of these complexes each showed a downfield chemical shift for ring-hydrogen H^6 of the pyS and pymS ligands, which suggests the ligands are attached to the metal in these complexes. Moreover, the inequivalence of the pymS ring-hydrogens H^4 and H^6, in complexes (**4–6**), infers bonding in the chelate mode for the pymS ligand. Magnetic susceptibility measurements on complexes (**2**) and (**5**) showed them to be diamagnetic, which is consistent with these compounds obeying the effective atomic number rule. Since the complex $[W(CO)_3(\eta^2\text{-pymS})_2]$ has a capped trigonal prismatic geometry, it may be that the structure of our N ∧ S chelate complexes (**2–7**) have a similar structure as shown in Fig. 2, and this is supported by infrared and ^1H NMR studies.

The tungsten complexes $[WI_2(CO)_3LL']$ (L = L' = PPh_3, PPh_2Cy or PPh_2Nap; L = PPh_3, L' = PPh_2Bz, $PPhBz_2$, $AsPh_3$ or $SbPh_3$; L = $PPhBz_2$, L' = $AsPh_3$) prepared either by reacting $[WI_2(CO)_3(NCMe)_2]$ with

Table 3
^{1}H NMR data (δ, J in Hz) [a] for the pyridine-2-thionate and pyrimidine-2-thionate complexes of molybdenum(II) and tungsten(II)

Complex	^{1}H(δ) ppm
pymS	8.50 (d, 2H, pymS–H^4, pymS–H^6, J_{HH} = 7 Hz); 6.95 (t, 1H, pymS–H^5, J_{HH} = 7 Hz)
pyS	8.50 (d, 1H, pyS–H^6, J_{HH} = 7 Hz); 7.65 (m, 2H, pyS–H^3, pyS–H^4); 7.10 (t, 1H, pyS–H^5, J_{HH} = 7 Hz)
1	8.60 (m, 2H, pymS–H^6); 8.45 (m, 2H, pymS–H^4); 6.95 (t, 2H, pymS–H^5, J_{HH} = 7 Hz)
2	8.75 (d, 1H, pyS–H^6); 7.90–7.50 (m, 17H, Ph–H, pyS–H^3, pyS–H^4); 6.90 (t, 1H, pyS–H^5, J_{HH} = 7.1 Hz)
3	8.80 (d, 1H, pyS–H^6); 7.92–7.50 (m, 17H, Ph–H, pyS–H^3, pyS–H^4); 7.10 (t, 1H, pyS–H^5, J_{HH} = 7.2 Hz)
4	8.80 (d, 1H, pymS–H^6, J_{HH} = 7 Hz); 8.05 (m, 1H, pymS–H^4); 7.40–7.25 (m, 15H, Ph–H); 6.80 (t, 1H, pymS–H^5, J_{HH} = 7.1 Hz)
5	8.90 (m, 1H, pymS–H^6); 8.05 (m, 1H, pymS–H^4); 7.50–7.25 (m, 15H, Ph–H); 6.85 (t, 1H, pymS–H^5, J_{HH} = 7 Hz)
6	8.60 (m, 1H, pymS–H^6); 8.05 (m, 1H, pymS–H^4); 7.70–7.30 (m, 10H, Ph–H); 6.55 (t, 1H, pymS–H^5, J_{HH} = 7.1 Hz); 1.80–1.20 (brm, 11H, Cy–H)
7	9.35 (m, 1H, pymS–H^6); 8.55 (m, 1H, pymS–H^4); 7.90–7.25 (m, 17H, Ph–H, Nap–H); 7.10 (t, 1H, pymS–H^5, J_{HH} = 7 Hz)
8	8.90 (m, pymS–H); 8.05 (m, pymS–H); 7.85 (m, pymS–H); 7.50–7.25 (m, 30H, Ph–H); 6.85 (t, pymS–H, J_{HH} = 7.1 Hz); 6.25 (t, pymS–H, J_{HH} = 7.1 Hz)
9	8.45 (m, 1H, pymS–H^6); 7.90 (m, 1H, pymS–H^4); 7.70–7.20 (m, 20H, Ph–H); 6.45 (t, 1H, pymS–H^5, J_{HH} = 7 Hz); 1.70–1.10 (brm, 22H, Cy–H)
10	8.35 (d, 1H, pymS–H^6, J_{HH} = 10 Hz); 7.85 (d, 1H, pymS–H^4, J_{HH} = 10 Hz); 7.75–7.15 (m, 34H, Ph–H, Nap–H); 6.85 (dd, 1H, pymS–H^5, J_{HH} = 4 Hz, 7 Hz)
11	8.85 (m, 1H, pymS–H^6); 8.00 (m, 1H, pymS–H^4); 7.70–7.20 (m, 30H, Ph–H, Bz–H); 6.80 (m, 1H, pymS–H^5); 2.35 (brs, 2H, CH_2Ph)
12	8.90 (m, 1H, pymS–H^6); 8.10 (m, 1H, pymS–H^4); 7.70–7.20 (m, 30H, Ph–H, Bz–H); 6.85 (t, 1H, pymS–H^5, J_{HH} = 7 Hz); 2.9 (brs, 4H, CH_2Ph)
13	9.05 (m, 1H, pymS–H^6); 8.25 (m, 1H, pymS–H^4); 7.68–7.40 (m, 30H, Ph–H); 7.05 (t, 1H, pymS–H^5, J_{HH} = 7 Hz)
14	8.90 (m, 1H, pymS–H^6); 8.10 (m, 1H, pymS–H^4); 7.50–7.25 (m, 30H, Ph–H); 6.85 (t, 1H, pymS–H^5, J_{HH} = 7.1 Hz)
15	8.60 (m, 1H, pymS–H^6); 8.90 (m, 1H, pymS–H^4); 7.50–7.20 (m, 30H, Ph–H, Bz–H); 6.90 (m, 1H, pymS–H^5); 2.85 (brs, 4H, CH_2Ph)
16	7.90 (d, 1H, pyS–H^6, J_{HH} = 7 Hz); 7.70 (t, 1H, pyS–H^4); 7.50–7.15 (m, 20H, Ph–H); 7.00 (m, 1H, pyS–H^5); 6.50 (d, 1H, pyS–H^3, J_{HH} = 9 Hz); 1.15 (s, 2H, PCH_2)
17	9.50 (m, 1H, pymS–H^6); 8.30 (m, 1H, pymS–H^4); 7.75–7.35 (m, 20H, Ph–H); 6.85 (t, 1H, pymS–H^5, J_{HH} = 7.1 Hz); 5.30 (s, 1H CH_2Cl_2); 4.55 (t, 2H, PCH_2, J_{PH} = 10.7 Hz)
18	7.90–7.20 (m, 21H, Ph–H, pyS–H^6); 6.95 (t, 1H, pyS–H^4, J_{HH} = 9 Hz); 6.55 (t, 1H, pyS–H^5, J_{HH} = 7 Hz); 6.25 (d, 1H, pyS–H^3, J_{HH} = 10 Hz); 1.65 (brm, 4H, PCH_2)
19	8.15 (m, 1H, pymS–H^6); 7.90 (m, 1H, pymS–H^4); 7.50–7.30 (m, 20H, Ph–H); 6.70 (t, 1H, pymS–H^5, J_{HH} = 7 Hz); 1.25 (m, 4H, PCH_2)
20	7.80–7.20 (m, 21H, Ph–H, pyS–H^6); 7.00 (t, 1H, pyS–H^4, J_{HH} = 8.9 Hz); 6.40 (d, 1H, pyS–H^3, J_{HH} = 8 Hz); 6.30 (t, 1H, pyS–H^5, J_{HH} = 7 Hz); 1.75 (brm, 4H, PCH_2CH_2); 1.25 (s, 2H, PCH_2CH_2)
21	8.15 (m, 1H, pymS–H^6); 7.80–7.20 (m, 21H, Ph–H, pymS–H^4); 6.40 (t, 1H, pymS–H^5, J_{HH} = 7 Hz); 1.85 (br s, 4H, PCH_2CH_2); 1.35 (s, 2H, PCH_2CH_2)
22	8.65 (m, 1H, pyS–H^6); 7.90–7.30 (m, 21H, Ph–H, pyS–H^4); 6.75 (m, 1H, pyS–H^5); 6.05 (d, 1H, pyS–H^3, J_{HH} = 9 Hz); 1.80 (brm, 4H, PCH_2CH_2); 1.35 (m, 4H, PCH_2CH_2)
23	8.05 (m, 1H, pymS–H^6); 7.80–7.20 (m, 21H, Ph–H, pymS–H^4); 6.60 (t, 1H, pymS–H^5, J_{HH} = 7 Hz); 1.50 (m, 4H, PCH_2CH_2); 1.25 (m, 4H, PCH_2CH_2)
24	8.70 (m, pyS–H^6); 7.90–7.10 (m, Ph–H, pyS–H^4); 6.80 (m, pyS–H^5); 6.25 (t, pyS–H^5, J_{HH} = 7 Hz); 6.15 (m, pyS–H^3); 5.95 (d, pyS–H^3, J_{HH} = 8.5 Hz); 2.50–1.40 (m, PCH_2CH_2CH_2)
25	8.50 (m, 1H, pymS–H^6); 7.85 (m, 1H, pymS–H^4); 7.40–7.10 (m, 20H, Ph–H); 6.40 (t, 1H, pymS–H^5, J_{HH} = 7 Hz); 2.15 (brm, 4H, PCH_2CH_2CH_2); 1.45–0.90 (brm, 6H, PCH_2CH_2CH_2CH_2)
26	8.60 (m, pyS–H^6); 7.90–7.00 (m, Ph–H, pyS–H^5); 6.85 (t, pyS–H^5, J_{HH} = 7.5 Hz); 6.65 (t, pyS–H^5, J_{HH} = 7.5 Hz); 6.05 (d, pyS–H^3, J_{HH} = 8.9 Hz); 5.90 (d, pyS–H^3); 5.40 (s, 1H, CH_2Cl_2); 3.00 (m, PCH_2CH_2CH_2); 2.30 (brs, PCH_2CH_2CH_2); 1.60–1.20 (brm, PCH_2CH_2CH_2)
27	8.65 (m, pymS–H^6); 8.05 (m, pymS–H^6); 7.80 (m, pymS–H^4); 7.60–7.25 (m, Ph–H); 6.55 (t, pymS–H^5, J_{HH} = 7 Hz); 5.30 (s, 1H, CH_2Cl_2); 2.85 (brm, PCH_2CH_2CH_2); 1.60–1.10 (brm, PCH_2CH_2CH_2)
28	8.95 (m, pymS–H^6); 8.30 (m, pymS–H^4); 8.15 (m, pymS–H^6); 7.85 (m, pymS–H^4); 7.60–7.25 (m, 20H, Ph–H); 6.85 (t, pymS–H^5, J_{HH} = 7 Hz); 6.60 (t, pymS–H^5, J_{HH} = 7 Hz); 1.25 (s, 2H, PCH_2); 0.85 (m, 2H, PCH_2)

[a] Spectra recorded in $CDCl_3$ (25°C) referenced to $SiMe_4$. s = singlet, d = doublet, t = triplet, m = multiplet, br = broad.

Table 4
Atomic coordinates ($\times 10^4$) and equivalent isotropic displacement parameters ($Å^2 \times 10^3$) for $[W(CO)_3(C_4H_3N_2S)_2]$

	x	y	z	U_{eq} [a]
W(1)	1970.6(3)	1817.2(2)	2675.1(3)	31.0(1)
S(1)	316(2)	1481(2)	476(2)	45(1)
S(2)	2647(2)	1260(1)	4870(2)	41(1)
N(1)	−2192(7)	833(5)	623(6)	41(2)
N(2)	−220(6)	1263(4)	2438(5)	30(1)
N(3)	2562(7)	245(4)	3028(5)	29(1)
N(4)	3250(8)	−708(5)	4862(6)	45(2)
O(1)	317(7)	3834(4)	1915(8)	68(2)
O(2)	4322(10)	3402(5)	3976(9)	94(3)
O(3)	4334(10)	1696(7)	1498(10)	105(4)
C(1)	−850(8)	1148(5)	1220(6)	31(1)
C(2)	−2944(9)	631(5)	1346(8)	41(2)
C(3)	−2400(9)	745(6)	2595(7)	40(2)
C(4)	−1014(8)	1069(5)	3138(7)	35(2)
C(5)	2847(8)	139(5)	4235(6)	31(1)
C(6)	3362(10)	−1473(6)	4178(8)	50(2)
C(7)	3089(10)	−1431(6)	2943(8)	47(2)
C(8)	2690(9)	−544(6)	2380(7)	38(2)
C(9)	947(10)	3131(5)	2215(10)	50(2)
C(10)	3455(10)	2789(6)	3535(10)	60(3)
C(11)	3495(11)	1797(6)	1970(12)	63(3)

[a] U_{eq} is defined as one third of the trace of the orthogonalized U_{ij} tensor.

Table 5
Bond lengths (Å) and angles (deg) for $[W(CO)_3(C_4H_3N_2S)_2]$

W(1)–S(1)	2.536(2)	W(1)–S(2)	2.520(2)
W(1)–N(2)	2.233(6)	W(1)–N(3)	2.207(5)
W(1)–C(9)	2.024(8)	W(1)–C(10)	1.960(9)
W(1)–C(11)	1.984(10)	S(1)–C(1)	1.753(7)
S(2)–C(5)	1.733(7)	N(1)–C(1)	1.334(10)
N(1)–C(2)	1.352(10)	N(2)–C(1)	1.339(9)
N(2)–C(4)	1.360(9)	N(3)–C(5)	1.343(8)
N(3)–C(8)	1.344(8)	N(4)–C(6)	1.340(10)
N(4)–C(5)	1.341(8)	O(1)–C(9)	1.124(9)
O(2)–C(10)	1.174(11)	O(3)–C(11)	1.170(13)
C(2)–C(3)	1.368(11)	C(3)–C(4)	1.367(11)
C(6)–C(7)	1.370(12)	C(7)–C(8)	1.357(11)
C(10)–W(1)–C(11)	70.8(5)	C(10)–W(1)–C(9)	76.1(3)
C(11)–W(1)–C(9)	106.9(4)	C(10)–W(1)–N(3)	116.8(3)
C(11)–W(1)–N(3)	82.6(3)	C(9)–W(1)–N(3)	166.4(3)
C(10)–W(1)–N(2)	144.2(4)	C(11)–W(1)–N(2)	144.3(4)
C(9)–W(1)–N(2)	83.5(3)	N(3)–W(1)–N(2)	83.2(2)
C(10)–W(1)–S(2)	79.0(3)	C(11)–W(1)–S(2)	117.6(3)
C(9)–W(1)–S(2)	117.0(3)	N(3)–W(1)–S(2)	64.38(14)
N(2)–W(1)–S(2)	84.7(2)	C(10)–W(1)–S(1)	136.7(3)
C(11)–W(1)–S(1)	83.5(4)	C(9)–W(1)–S(1)	79.1(3)
N(3)–W(1)–S(1)	92.7(2)	N(2)–W(1)–S(1)	64.7(2)
S(2)–W(1)–S(1)	144.20(7)	C(1)–S(1)–W(1)	81.1(3)
C(5)–S(2)–W(1)	81.7(2)	C(1)–N(1)–C(2)	114.9(7)
C(1)–N(2)–C(4)	118.1(6)	C(1)–N(2)–W(1)	103.0(4)
C(4)–N(2)–W(1)	138.9(5)	C(5)–N(3)–C(8)	118.8(6)
C(5)–N(3)–W(1)	103.8(4)	C(8)–N(3)–W(1)	137.4(5)
C(6)–N(4)–C(5)	114.1(7)	N(1)–C(1)–N(2)	125.6(6)
N(1)–C(1)–S(1)	123.1(6)	N(2)–C(1)–S(1)	111.3(5)
N(1)–C(2)–C(3)	123.6(7)	C(4)–C(3)–C(2)	117.9(7)
N(2)–C(4)–C(3)	119.9(7)	N(4)–C(5)–N(3)	124.9(6)
N(4)–C(5)–S(2)	124.9(6)	N(3)–C(5)–S(2)	110.1(5)
N(4)–C(6)–C(7)	124.8(7)	C(8)–C(7)–C(6)	117.3(7)
N(3)–C(8)–C(7)	120.1(7)	O(1)–C(9)–W(1)	176.3(8)
O(2)–C(10)–W(1)	175.5(9)	O(3)–C(11)–W(1)	173.1(11)

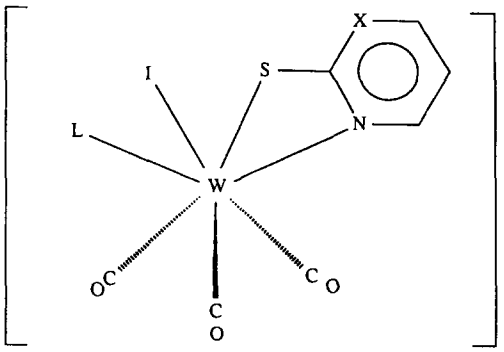

X = CH or N

Fig. 2. Proposed structure for $[WI(CO)_3L(\eta^2\text{-pyS or pymS})]$ (**2–7**).

two equivalents of L = L′, [21] or one equivalent of L followed by an equimolar amount of L′, [22] in CH_2Cl_2 at room temperature. These $[WI_2(CO)_3LL']$ complexes (prepared in situ) when treated with an equimolar amount of K[pymS] yielded the S-bonded monodentately attached pyrimidine-2-thionate complexes $[WI(CO)_3LL'(\eta^1\text{-S-pymS})]$ (**8–15**) in good yield. These complexes were characterised by elemental analysis (C, H and N) (Table 1), IR spectroscopy (Table 2), ^1H NMR spectroscopy (Table 3) and in selected cases, molar conductivity measurements (Table 6). All of these new complexes were fairly stable in the solid-state when kept under dinitrogen, but slowly decomposed in solution when exposed to air. These complexes were all soluble in acetone and chlorinated solvents, but were only sparingly soluble in diethyl ether and insoluble in hydrocarbon solvents. The IR spectra of these complexes were consistent with their being tricarbonyl complexes (Table 2). The ^1H NMR spectra were consistent with two of L(L′) and one equivalent of pymS being present in these complexes. The downfield chemical shift of ring-proton H^6 of the pymS ligand in most of these complexes with respect to the uncoordinated ligand, suggests coordination of pymS. The ^1H NMR spectra of a number of these complexes suggested the presence of isomers in solution. The molar conductivities of (**10**) and (**11**) (Table 6) show them to be essentially nonelectrolytes as expected and confirm the monodentate coordination of the pyrimidine-2-thionate ligands. Magnetic susceptibility measurements for complexes (**11**) and (**12**) suggest that they are diamagnetic and coordinatively saturated. Several unsuccessful attempts were made to grow suitable single crystals of several complexes for X-ray crystallography. It should be noted that several attempts to prepare the analogous pyridine-2-thionate complexes were also unsuccessful, and although reactions occurred the products could not be isolated in a pure state. Also, attempts to prepare the analogous molybdenum(II) complexes of this type were

Table 6
Molar conductance [a] for selected pyridine-2-thionate and pyrimidine-2-thionate complexes of molybdenum(II) and tungsten(II)

Complex	Molar conductance (10^4 m^2 Ω^{-1} mol^{-1})
10	20
11	40
18	16
21	16
28	33

[a] Measurements are for a 1×10^{-3} mol dm^{-3} concentration in acetone under dinitrogen at 25°C.

unsuccessful. They were considerably less stable than their tungsten analogues.

Equimolar quantities of $[MI_2(CO)_3(NCMe)_2]$ and $Ph_2P(CH_2)_nPPh_2$ (for M = W, $n = 1$–6; for M = Mo, $n = 2$) react in CH_2Cl_2 at room temperature to give $[MI_2(CO)_3\{Ph_2P(CH_2)_nPPh_2\}]$ [23] which when treated in situ with an equimolar amount of K[pyS] or K[pymS] affords the S-monodentately attached tungsten complexes $[WI(CO)_3\{Ph_2P(CH_2)PPh_2\}(\eta^1$-S-pyS or -S-pymS)] (**16–27**) or the bidentately attached pyrimidine-2-thionate molybdenum complex $[MoI(CO)_2\{Ph_2P(CH_2)_2PPh_2\}(\eta^2$-pymS)] (**28**) in good yield. The complexes were characterised in the normal manner (see Tables 1–3). Tungsten analyses for complexes (**21**) and (**22**) and iodine analysis for complexes (**16**), (**18**) and (**23**) were also obtained (see Table 1). Complexes (**17**), (**26**) and (**27**) were also confirmed as CH_2Cl_2 solvates by repeated elemental analyses and ^1H NMR spectroscopy (Table 3). As is usual for this type of complex, they are stable when stored under dinitrogen, but decompose when exposed to air in solution, and, more slowly, in the solid state. Like other complexes described in this paper, the complexes were all soluble in acetone and CH_2Cl_2, but only slightly soluble in diethyl ether and insoluble in hydrocarbon solvents. As expected, the tungsten complexes (**16** → **27**) all have three carbonyl bands in their IR spectra, whereas the molybdenum complex $[MoI(CO)_2\{Ph_2P(CH_2)_2PPh_2\}(\eta^2$-pymS)] has the expected two carbonyl bands at 1957 and 1885 cm^{-1}. The relative ease of decarbonylation of molybdenum(II) carbonyl complexes compared with that of their tungsten(II) analogues is well known. The molar conductivities of complexes (**18**), (**21**) and (**28**) (Table 6) have values which suggest the complexes are, as proposed, neutral complexes with monodentate coordination of the pyS or pymS ligands. The ^1H NMR spectra of the complexes (Table 3) are, again suggesting the presence of isomers in solution. Magnetic susceptibility measurements on complexes (**17**), (**25**), (**26**) and (**28**) show that the complexes are, as expected diamagnetic, and hence obey the effective atomic number rule.

3. Experimental details

The synthesis and purification of the complexes were carried out under dry dinitrogen by use of standard Schlenk-line techniques. The solvent, CH_2Cl_2 was dried over phosphorus pentoxide (P_4O_{10}), distilled, and degassed before use. The starting complexes $[MI_2(CO)_3(NCMe)_2]$ (M = Mo or W) were synthesised according to the literature method [10]. The potassium salts of pyridine-2-thionate and pyrimidine-2-thionate were prepared by reaction of equimolar quantities of the thiones and KOH in methanol. The phosphines, PPh_2Cy, PPh_2Bz (Bz = benzyl), $PPhBz_2$ and PPh_2Nap (Nap = napthyl) were prepared by standard methods. All other chemicals were purchased from commercial sources and used without further purification.

Elemental analyses (C, H and N) were carried out with a Carlo Erba Elemental Analyser MOD 1106 with helium as the carrier gas. Iodine content was determined by allowing a sample of each (selected) complex to decompose in an acetone/0.1 M $NaHCO_3$ mixture (1 : 20) during a period of 7 d. The amount of (displaced) iodide ion was then measured by Chemically-Suppressed Ion Chromatography using a Dionex 2000 i/SP Ion Chromatography System with conductivity detection. An IonPac AS4A Analytical Column was used for the separation of anions. The column comprised of 15 micron polystyrene/divinyl benzene substrate agglomerated with fully aminated anion exchange latex. A mixture of aqueous $NaHCO_3$ (1.7 mM) and Na_2CO_3 (1.8 mM) was used as eluant, at a flow rate of 2 ml min^{-1}, for the separation and elution of iodide. Potassium iodide was used for the preparation of standards for calibration. All standards and samples were prepared in the same matrix (0.1M $NaHCO_3$). Tungsten was determined, for the acid-digested complex, in solution by Flame Atomic Absorption Spectrometry using a Thermo Jarrell Ash Video 11E atomic absorption spectrophotometer; a wavelength of 255.1 nm was used with Smith–Hieftje ('pulsing-lamp') background correction. A fuel-rich nitrous-oxide–acetylene (N_2O/C_2H_2) flame was used for atomisation. Merck 'Spectrosol' standard tungsten solution (1000 mg dm^{-3}) was used as a stock solution for the preparation of standard solutions. All standard solutions, samples and blank solutions were prepared in identical acid matrix.

^1H and ^{13}C NMR spectra were recorded on a Bruker AC250 (^1H) NMR spectrometer or a Bruker WH400 (^{13}C) NMR spectrometer referenced against tetramethylsilane as the internal standard. All IR spectra were recorded as thin films between NaCl plates, on a Perkin Elmer 1600 FTIR spectrophotometer. Molar conductances were measured at 25°C with a standard laboratory conductivity meter, Jenway model 4070, referenced against a 1×10^{-3} M solution of KCl; solutions were in acetone under dinitrogen. Magnetic susceptibilities were

measured with Johnson Matthey magnetic susceptibility balance.

3.1. $[W(CO)_3(\eta^2\text{-pymS})_2]$ (1)

To $[WI_2(CO)_3(NCMe)_2]$ (0.5 g, 0.828 mmol) dissolved in CH_2Cl_2 (15 cm^3), with continuous stirring under a stream of dry dinitrogen was added K[pymS] (0.249 g, 1.656 mmol). After 18 h, the solution was filtered to remove KI. Removal of the solvent in vacuo afforded a dark-brown solid which on recrystallisation from CH_2Cl_2–Et_2O gave $[W(CO)_3(\eta^2\text{-pymS})_2]$ (**1**) (yield of pure product = 0.31 g, 76%).

A sample of the pure complex was dissolved in a minimum volume of CH_2Cl_2 to which was added a volume of diethyl ether (20 : 80 ratio), which was cooled at −25°C for four weeks to yield amber-coloured single crystals, suitable for X-ray crystallography. For physical and analytical data see Table 1.

3.2. $[WI(CO)_3(PPh_3)(\eta^2\text{-pyS})]$ (3)

To $[WI_2(CO)_3(NCMe)_2]$ (0.5 g, 0.828 mmol) dissolved in CH_2Cl_2 (15 cm^3), continuous stirring under a stream of dry dinitrogen was added PPh_3 (0.217 g, 0.828 mmol). The solution turned yellow. After 10 min K[pyS] was added (0.124 g, 0.828 mmol). The solution turned dark-brown. After 2 h the solution was filtered to remove KI and other insoluble material. Removal of solvent in vacuo afforded a dark-brown solid, which on recrystallisation from CH_2Cl_2–Et_2O gave a brown solid $[WI(CO)_3(PPh_3)(\eta^2\text{-pyS})]$ (**3**); (yield of pure product = 0.35 g, 55%).

Similar reaction of $[MoI_2(CO)_3(NCMe)_2]$ with an equimolar amount of PPh_3 in CH_2Cl_2 at room temperature, followed by one equivalent of K[pyS] gave $[MoI(CO)_3(PPh_3)(\eta^2\text{-pyS})]$ (**2**). For physical and analytical data see Table 1.

3.3. $[MoI(CO)_3(PPh_3)(\eta^2\text{-pymS})]$ (4)

To $[MoI(CO)_3(NCMe)_2]$ (0.5 g, 0.969 mmol) dissolved in CH_2Cl_2 (15 cm^3) with continuous stirring, under a stream of dry dinitrogen was added PPh_3 (0.254 g, 0.969 mmol). After 20 min K[pymS] (0.145 g, 0.969 mmol) was added. The solution was stirred for a further 3 h and then filtered to remove KI and other insoluble material. Removal of solvent in vacuo afforded a dark purple–brown solid, which on recrystallisation from CH_2Cl_2–Et_2O gave a dark purple–brown solid $[MoI(CO)_3(PPh_3)(\eta^2\text{-pymS})]$ (**4**) (yield of pure product = 0.47 g, 71%).

3.4. $[WI(CO)_3(PPh_3)(\eta^2\text{-pymS})]$ (5)

To $[WI_2(CO)_3(NCMe)_2]$ (0.5 g, 0.828 mmol) dissolved in CH_2Cl_2 (15 cm^3), with continuous stirring under a stream of dry dinitrogen, was added PPh_3 (0.217 g, 0.828 mmol). The solution turned yellow. After 10 min K[pymS] (0.124 g, 0.828 mmol) was added. The solution turned brown. After 2 h the solution was filtered to remove KI and other insoluble material. Removal of the solvent in vacuo afforded a brown solid which on recrystallisation from CH_2Cl_2–Et_2O yielded a brown solid $[WI(CO)_3(PPh_3)(\eta^2\text{-pymS})]$ (**5**) (yield of pure product = 0.39 g, 61%).

Similar reactions of $[WI_2(CO)_3(NCMe)_2]$ with an equimolar amount of L (L = PPh_2Cy or PPh_2Nap) in CH_2Cl_2 at room temperature give $[WI_2(CO)_3(NCMe)L]$, followed by treatment with K[pymS] gave $[WI(CO)_3L(\eta^2\text{-pymS})]$ (**6** and **7**). For physical and analytical data see Table 1.

3.5. $[WI(CO)_3(PPh_3)_2(\eta^1\text{-pymS})]$ (8)

To $[WI_2(CO)_3(NCMe)_2]$ (0.5 g, 0.828 mmol) dissolved in CH_2Cl_2 (15 cm^3), with continuous stirring, under a stream of dry dinitrogen, was added PPh_3 (0.434 g, 1.656 mmol). The solution turned yellow-green. After 20 min K[pymS] (0.124 g, 0.828 mmol) was added. The solution turned brown. After 3 h the solution was filtered to remove KI and other insoluble material. Removal of the solvent in vacuo afforded a brown solid, which on recrystallisation from CH_2Cl_2–Et_2O gave an orange solid $[WI(CO)_3(PPh_3)_2(\eta^1\text{-pymS})]$ (**8**) (yield of pure product = 0.43 g, 50%).

Similar reactions of $[WI_2(CO)_3(NCMe)_2]$ with two equivalents of L (L = PPh_2Cy or PPh_2Nap) in CH_2Cl_2 at room temperature to give $[WI_2(CO)_3L_2]$ followed by reaction with K[pymS] gave $[WI(CO_3)L_2(\eta^1\text{-pymS})]$ (**9–10**). For physical and analytical data see Table 1.

3.6. $[WI(CO)_3(PPh_3)(SbPh_3)(\eta^1\text{-pymS})]$ (14)

To $[WI_2(CO)_3(NCMe)_2]$ (0.5 g, 0.828 mmol) dissolved in CH_2Cl_2 (15 cm^3) with continuous stirring under a stream of dry dinitrogen was added PPh_3 (0.217 g, 0.828 mmol). After 10 min, $SbPh_3$ was added (0.292 g, 0.828 mmol). The solution turned orange–red. After a further 20 min, K[pymS] (0.124 g, 0.828 mmol) was added. After 3 h the solution was filtered to remove KI and other insoluble material. Removal of the solvent in vacuo gave a dark-brown, oil, which was crystallised from CH_2Cl_2–Et_2O to afford a dark-brown solid $[WI(CO)_3(PPh_3)(SbPh_3)(\eta^1\text{-pymS})]$ (**14**); (yield of pure product = 0.3 g, 32%).

Similar reactions of $[WI_2(CO)_3(NCMe)_2]$ with an equimolar quantity of L (L = PPh_3 or $PPhBz_2$) in CH_2Cl_2 at room temperature, followed by an in situ reaction with L′ (for L = PPh_3, L′ = PPh_2Bz, $PPhBz_2$ or $AsPh_3$; for L = $PPhBz_2$, L′ = $AsPh_3$) gave $[WI_2(CO)_3LL']$, which when also reacted in situ with one equivalent of K[pymS] gave $[WI(CO)_3LL'(\eta^1\text{-pymS})]$

(**11**, **12**, **13** and **15**). For physical and analytical data see Table 1.

3.7. [WI(CO)$_3$(dppm)(η^1-pyS)] (16)

To [WI$_2$(CO)$_3$(NCMe)$_2$] (0.5 g, 0.828 mmol) dissolved in CH_2Cl_2 (15 cm^3), with continuous stirring under a stream of dry dinitrogen was added dppm (0.318 g, 0.828 mmol). The solution turned orange–red. After 10 min, K[pyS] (0.124 g, 0.828 mmol) was added. The solution gradually turned brown. After 2 h, the solution was filtered to remove KI and other insoluble material. Removal of solvent in vacuo afforded a brown solid as the crude product, which was recrystallised from CH_2Cl_2–Et_2O to give a golden-brown solid [WI(CO)$_3$(dppm)(η^1-pyS)] (**16**); (yield of pure product = 0.61 g, 83%).

Similar reactions of [WI$_2$(CO)$_3$(NCMe)$_2$] with an equimolar amount of $Ph_2P(CH_2)_nPPh_2$ (n = 2–6) in CH_2Cl_2 at room temperature give [WI$_2$(CO)$_3${Ph_2P-$(CH_2)_nPPh_2$}], followed by an in situ reaction with K[pyS] gave [WI(CO)$_3${$Ph_2P(CH_2)_nPPh_2$}(η^1-pyS)] (**18**), (**20**), (**22**), (**24**) and (**26**). For physical and analytical data see Table 1.

3.8. [WI(CO)$_3$(dppm)(η^1-pymS)] · $\frac{1}{2}CH_2Cl_2$ (17)

To [WI$_2$(CO)$_3$(NCMe)$_2$] (0.5 g, 0.828 mmol) dissolved in CH_2Cl_2 (15 cm^3), with continuous stirring under a stream of dry dinitrogen was added dppm (0.318 g, 0.828 mmol). The solution turned orange–red. After 10 min, K[pymS] (0.124 g, 0.828 mmol) was added in situ. After 2 h, the solution was filtered to remove KI and other insoluble material. Removal of solvent in vacuo afforded a brown solid which was recrystallised from CH_2Cl_2–Et_2O to give [WI(CO)$_3$-(dppm)(η^1-pymS)]$\frac{1}{2}CH_2Cl_2$ (**17**) (yield of pure product = 0.55 g, 71%).

Similar reactions of [WI$_2$(CO)$_3$(NCMe)$_2$] with an equimolar amount of $Ph_2P(CH_2)_nPPh_2$ (n = 2–6) in CH_2Cl_2 at room temperature to give [WI$_2$(CO)$_3${Ph_2P-$(CH_2)_nPPh_2$}], followed by an in situ reaction with K[pymS] gave [WI(CO)$_3${$Ph_2P(CH_2)_nPPh_2$}(η^1-pymS)] (**19**), (**21**), (**23**), (**25**) and (**27**). For physical and analytical data see Table 1.

3.9. [MoI(CO)$_2$(dppe)(η^2-pymS)] (28)

To [MoI$_2$(CO)$_3$(NCMe)$_2$] (0.5 g, 0.969 mmol) dissolved in CH_2Cl_2, with continuous stirring under a stream of dry dinitrogen, was added dppe (0.386 g, 0.969 mmol). After 10 min K[pymS] (0.146 g, 0.969 mmol) was added. After 2 h the solution was filtered to remove KI and other insoluble material. Removal of solvent in vacuo afforded a brown solid as crude product, which was recrystallised from CH_2Cl_2–Et_2O to give [MoI(CO)$_2$(dppe)(η^2-pymS)] (**28**) (yield of pure product = 0.33 g, 43%).

3.10. X-ray crystallography

Crystals of (**1**) suitable for X-ray work were prepared as described above.

3.10.1. Crystal data

$C_{11}H_6N_4O_3S_2W$, M = 490.17, monoclinic, a = 9.996(4), b = 13.540(2), c = 11.713(1) Å, β = 111.68(1)°, U = 1473.2(6) Å^3 (by least squares refinement of diffractometer angles for 250 reflections within θ = 2.2°–30.0°, λ = 0.71069 Å), space group $P2_1/c$, Z = 4, Dc = 2.210 g cm^{-3}, $F(000)$ = 920, μ = 81.4 cm^{-1}, T = 293 K, orange blocks, crystal size 0.30 × 0.15 × 0.12 mm^3.

3.10.2. Data collection and processing [24]

Delft Instruments FAST TV area detector diffractometer positioned at the window of rotating anode generator, Mo-Kα radiation; 7850 reflections measured ($2.2 < \theta < 30.0°$; index ranges $-13 < h < 10$; $-18 < k < 17$; $-15 < l < 12$), 3783 unique {merging R = 0.0683 after absorption correction (max. and min. absorption correction factors = 0.899, 1.167)}.

3.10.3. Structure analysis and refinement

The structure was solved by the routine heavy atom procedures. Full-matrix least squares refinement on F^2 with all nonhydrogen atoms anisotropic and hydrogen atoms (in idealised positions) isotropic. Weighting scheme $w = 1/\sigma^2(Fo)^2$ was used which gave satisfactory agreement analyses. Final wR_2 ($= [\Sigma\{w(\Delta(F^2)^2)\}/\Sigma\{w(Fo^2)^2\}]^{1/2}$) and R_1[$= \Sigma(\Delta F)/\Sigma(Fo)$] values are 0.1221 and 0.0557 respectively, for 196 parameters and all 3783 data {ρ_{min}, ρ_{max} −2.21, 2.33 e Å^{-3} (near the W atom); $(\Delta/\sigma)_{max}$ 0.004}. The corresponding wR_2 and R_1 values for 2780 data with $Fo > 4\sigma(Fo)$ are 0.1131 and 0.0456, respectively. All calculations were done on a 486DX2/66 personal computer using the programs SHELX-S [25] (solution), SHELXL-93 [26] (refinement) and DIFABS [27] (absorption correction). Sources of scattering factor data are given in Ref. [26].

The fractional coordinates of the nonhydrogen atoms and bond lengths and angles are given in Tables 4 and 5, respectively. Tables of anisotropic displacement parameters and hydrogen atom coordinates have been deposited at the Cambridge Crystallographic Data Centre.

Acknowledgements

S.H. thanks the Institute of Terrestrial Ecology for support. We thank the Open University S343 Summer

School students at the University of York for preparing the phosphine ligands, PPh_2Cy, PPh_2Bz, $PPhBz_2$ and PPh_2Nap. We also thank Dr. O.W. Howarth for obtaining the ^{13}C NMR spectra on the Bruker WH400 MHz NMR spectrometer on the SERC High Field NMR Service at the University of Warwick.

References

[1] D. Coucouvanis, *Prog. Inorg. Chem., 11* (1970) 233.
[2] D. Coucouvanis, *Prog. Inorg. Chem., 26* (1979) 301.
[3] R. Eisenberg, *Prog. Inorg. Chem., 12* (1970) 295.
[4] E.W. Abel, M.A. Bennett and G. Wilkinson, *J. Chem. Soc.*, (1959) 2323.
[5] A.J. Deeming, K.I. Hardcastle and M Nafees Meah, *J. Chem. Soc., Dalton Trans.*, (1988) 227.
[6] A.J. Deeming, M. Nafees Meah, N.P. Randle and K.I. Hardcastle, *J. Chem. Soc., Dalton Trans.*, (1989) 2211.
[7] N. Zhang, S.R. Wilson and P.A. Shapley, *Organometallics, 7* (1988) 1126.
[8] A. Castiñeiras, W. Hiller, J. Strähle, J. Bravo, J.S. Casas, M. Gayoso and J. Sordo, *J. Chem. Soc., Dalton Trans.*, (1986) 1945.
[9] A.J. Deeming, M. Karim and N.I. Powell, *J. Chem. Soc., Dalton Trans.*, (1990) 2321.
[10] P.K. Baker, S.G. Fraser and E.M. Keys, *J. Organomet. Chem., 309* (1986) 319.
[11] D.P. Tate, W.R. Knipple and J.M. Augl, *Inorg. Chem., 1* (1962) 433.
[12] P.R. Traill, A.G. Wedd and E.R.T. Tiekink, *Aust. J. Chem., 45* (1992) 1933.
[13] M.L. Durán, J. Romero, J.A. García-Vázquez, R. Castro, A. Castiñeiras and A. Sousa, *Polyhedron, 10* (1991) 197.
[14] R. Castro, M.L. Durán, J.A. García-Vázquez, J. Romero, A. Sousa, A. Castiñeiras, W. Hiller and J. Strähle, *J. Chem. Soc., Dalton Trans.*, (1990) 531.
[15] J.L. Templeton and B.C. Ward, *Inorg. Chem., 19* (1980) 1753.
[16] J.L. Templeton and B.C. Ward, *J. Am. Chem. Soc., 103* (1981) 3743.
[17] R. Castro, M.L. Durán, J.A. García-Vázquez, J. Romero, A. Sousa, A. Castiñeiras, W. Hiller and J. Strähle, *Z. Naturforsch, Sect. B, 476* (1992) 1067.
[18] I.A. Latham, G.J. Leigh, C.J. Pickett, G. Huttner, I. Jibrill and J. Zubieta, *J. Chem. Soc., Dalton Trans.*, (1986) 1181.
[19] P.K. Baker and S.G. Fraser, *Transition Met. Chem., 12* (1987) 560.
[20] E. Spinner, *J. Chem. Soc.*, (1960) 1237.
[21] P.K. Baker and S.G. Fraser, *Inorg. Chim. Acta*, 116 (1986) L1.
[22] P.K. Baker, S.G. Fraser and M.G.B. Drew, *J. Chem. Soc., Dalton Trans.*, (1988) 2729.
[23] P.K. Baker and S.G. Fraser, *Inorg. Chim. Acta, 130* (1987) 61.
[24] J.A. Darr, S.R. Drake, M.B. Hursthouse and K.M.A. Malik, *Inorg. Chem., 32* (1993) 5704.
[25] G.M. Sheldrick, *Acta Crystallogr., A46* (1990) 467.
[26] G.M. Sheldrick, SHELEXL-93, program 4. Crystal Structure Refinement, University of Göttingen, Germany, 1993.
[27] N. Walker and D. Stuart, *Acta Crystallogr., A39* (1983) 158; adapted for FAST geometry by A.I. Karaulov, University of Wales, 1991.